

Seasonality of interbasin SST contributions to Atlantic tropical cyclone activity

Robert West^{1,2}, Hosmay Lopez², Sang-Ki Lee², Andrew E. Mercer^{1,3}, Dongmin Kim^{2,4}, Gregory R. Foltz² and Karthik Balaguru⁵

¹Northern Gulf Institute, Mississippi State University, Mississippi State, MS, USA

²NOAA/Atlantic Oceanographic and Meteorological Laboratory, Miami, FL, USA

³Department of Geosciences, Mississippi State University, Mississippi State, MS, USA

⁴Cooperative Institute for Marine and Atmospheric Studies, University of Miami, Miami, FL, USA

⁵Pacific Northwest National Laboratory, Richland, WA, USA

Corresponding author: Robert West (robert.west@noaa.gov), NOAA/Atlantic Oceanographic and Meteorological Laboratory, 4301 Rickenbacker Cswy, Miami, FL 33149 USA

Key Points:

- This study explores the seasonality of Pacific and Atlantic SST contributions to Atlantic hurricane activity
- Early-season hurricane activity is largely influenced by Atlantic SSTAs, but Pacific SSTAs are equally important in the late-season
- An interbasin SST index is a reliable predictor of seasonal hurricane activity, albeit the Atlantic SST is a limiting factor

Abstract

Recent studies have demonstrated that the difference in sea surface temperature anomalies (SSTAs) between the tropical Atlantic main development region (MDR) and the tropical Pacific (Niño 3) modulates Atlantic tropical cyclone activity. This study further explores the seasonality of Pacific and Atlantic contributions to Atlantic hurricane activity. Our analysis shows that while MDR and Niño 3 SSTAs are equally important for late-season (September–November) activity, early-season (June–August) activity is largely modulated by MDR SSTAs. This reflects the increased (reduced) variance of MDR (Niño 3) SSTAs in the early-season due to their phase locking to the seasonal cycle. Further analysis yields skillful forecasts using an MDR–Niño 3 interbasin index derived from hindcasts of the North American Multi-Model Ensemble with May initial conditions. However, the prediction skill for MDR SSTAs is lower than that of Niño 3 SSTAs, suggesting that increasing the prediction skill for MDR SSTAs is key to improving seasonal outlooks.

Plain Language Summary

The difference in sea surface temperatures (SST) between the tropical Atlantic and the tropical Pacific changes atmospheric circulation patterns that affect Atlantic hurricane activity during the June–November Atlantic hurricane season. This study finds that tropical Atlantic SST have a stronger influence on hurricane activity in the early-season, but tropical Pacific and tropical Atlantic SST have equal influence in the late-season. This is because the seasonal variability of tropical Atlantic SST increases in the early-season, while the seasonal variability of tropical Pacific SST increases in the late-season, known as a seasonal phase locking mechanism. A statistical model of the differences in Atlantic and Pacific SST finds skillful forecasts of above-average hurricane activity throughout the hurricane season, with the greatest overall skill in the late-season.

1 Introduction

Tropical cyclone (TC) development frequently occurs in the main development region (MDR, 10°N–20°N, 60°W–20°W) located in the tropical North Atlantic Ocean and extreme eastern Caribbean Sea (Goldenberg & Shapiro, 1996; Landsea, 1993). Within the MDR, vertical wind shear (VWS) and convective instability are the dominant local environmental factors that influence TC activity (Gray, 1968; Shapiro, 1987; Emanuel, 1994; Goldenberg et al., 2001).

Environmental conditions within the MDR during the Atlantic hurricane season (June–November; JJASON) are strongly influenced by tropical atmosphere–ocean interannual variability. For instance, the El Niño–Southern Oscillation (ENSO) is well known to modulate Atlantic VWS and therefore TC development (Gray, 1984; Shapiro, 1987; Goldenberg &

Shapiro, 1996; Kossin et al., 2010; Klotzbach, 2011). Atlantic Warm Pool (AWP) amplitude and the Atlantic Meridional Mode (AMM) have been shown to correlate with Atlantic MDR TC activity (Wang et al., 2006; Vimont & Kossin, 2007; Xie et al., 2005). On decadal timescales, connections between Atlantic TC activity and the Atlantic Multidecadal Oscillation have been established (Goldenberg & Shapiro, 1996; Zhang & Delworth, 2006). Shifts in Atlantic TC activity as a result of anthropogenic climate change are a subject of ongoing research (Knutson et al., 2020).

The modulation of seasonal TC activity in the Atlantic is largely dictated by the relative SST difference between the (local) MDR and the (remote) tropical Pacific (Latif et al., 2007; Vecchi & Soden, 2007; Swanson, 2008; Vecchi et al., 2008; Wang & Lee, 2008; Lee et al., 2011). In the tropical Pacific, warm SSTAs support increased convection, which warms the global tropical troposphere through a fast tropical teleconnection (Yulaeva & Wallace, 1994; Chiang & Sobel, 2002). This in turn increases the meridional tropospheric temperature gradient across the edge of the tropics, which enhances VWS over the MDR via the thermal wind relationship and results in a less favorable environment for TC activity (Gray, 1984; Tang & Neelin, 2004; Lee et al., 2011; Larson et al., 2012). Differences in remote and local SST can also influence TC maximum potential intensity (Camargo et al., 2013; Swanson, 2008; Vecchi & Soden, 2007).

However, the relative SST influence on Atlantic TC activity may not be consistent throughout the hurricane season. Specifically, ENSO exhibits a strong phase locking to the seasonal cycle, where the amplitude of tropical central and eastern Pacific SSTAs reach a minimum in boreal spring and a maximum in November-December (Rasmusson & Carpenter, 1982; Wang & Fiedler, 2006). This suggests the remote influence of ENSO may be much weaker in the early-season (JJA) compared to the late-season (SON). In the tropical North Atlantic, the amplitude of

the AWP increases throughout the early season and typically reaches a maximum in September (Wang & Enfield, 2001), while AMM variance peaks in boreal spring but persists throughout JJASON (Vimont & Kossin, 2007). The enhanced early-season variability of tropical Atlantic SSTAs, relative to tropical Pacific SSTAs, indicates a relative increase in the influence of local SSTAs on early-season TC activity.

Consistent with this hypothesis, interannual variations in early- and late-season ACE are not highly correlated ($\rho = 0.44$, Figure S1), even in extremely active hurricane seasons (e.g., 2005 and 2017). Consequently, we explore the impacts of local and remote SSTAs on Atlantic TC activity during the early and late hurricane seasons. We additionally examine the seasonal predictability of Atlantic TC activity using remote and local SSTAs from hindcasts of the North American Multi-Model Ensemble (NMME).

We first describe the influence of local and remote SST on Atlantic TC activity during JJASON and identify the MDR and the Niño 3 region (5°N - 5°S , 150°W - 90°W) as the local and remote domains of greatest SSTAs impact (section 3). In section 4, changes in the relative impacts of MDR and Niño 3 SST from JJA to SON are investigated. Section 5 develops early- and late-season interbasin SST indices, which are implemented with NMME SSTAs in section 6 to determine the predictive skill of seasonal Atlantic TC activity.

2 Data

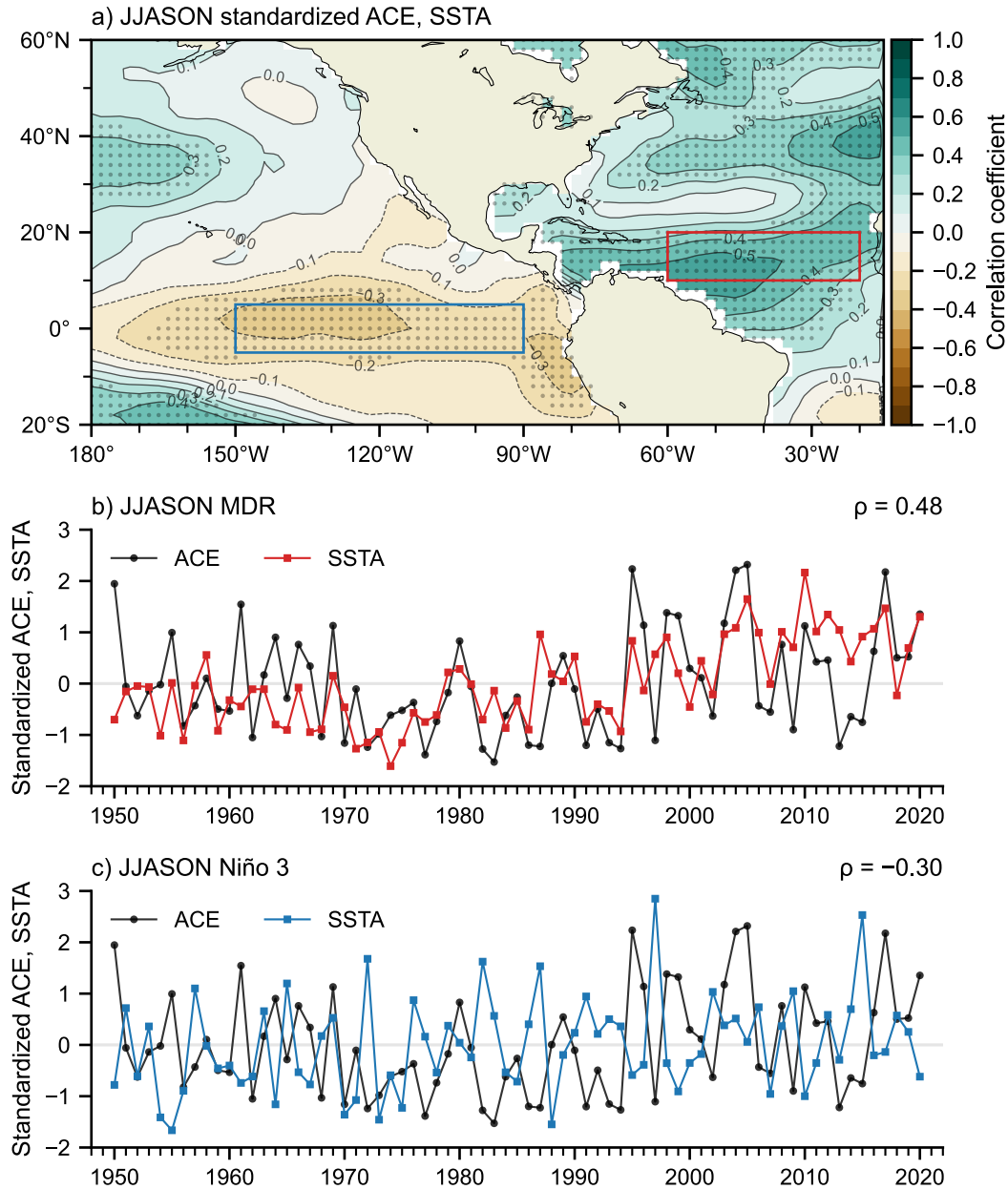
This study analyzes monthly SST from the Extended Reconstructed Sea Surface Temperature, version 5 (ERSSTv5) data set (Huang et al., 2017). Tropical cyclone data were obtained from the National Hurricane Center's (NHC) second-generation hurricane database (HURDAT2) (Landsea & Franklin, 2013). Atlantic tropical cyclone activity is measured using the accumulated cyclone energy index (ACE, units of kts^2), which is a metric of the number, strength and duration

of storms in a season (Bell et al., 2000). ACE is computed for each hurricane season by summing the squared maximum wind velocity every six hours for each tropical and subtropical cyclone that is of tropical storm or hurricane strength (sustained winds greater than 34 knots). ACE is standardized by removing the seasonal climatology and normalizing by the corresponding seasonal standard deviation. ERSSTv5 and ACE are examined from 1950-2020 (71 years) which only includes data obtained after Atlantic hurricane reconnaissance flights began to avoid undercounting open ocean TCs (Landsea, 2007).

We also use SST hindcasts from the NMME, a multi-agency seasonal prediction system which incorporates climate forecasts from several North American models (Kirtman et al., 2014). Eight models comprising 93 total ensemble members (see Table S1) from 1982-2009 (28 years) have been used. The hindcasts are initialized with May initial conditions and run to lead times spanning the Atlantic hurricane season.

3 The Local-Remote SST Relationship

Figure 1a explores the relationship between local and remote seasonally-averaged SSTAs and ACE during JJASON. MDR SSTAs show a statistically significant (at the 95% confidence level) positive correlation with ACE, with correlation coefficients (denoted by ρ) exceeding 0.5. The region of strongly positive ACE and SSTA correlation also extends throughout the Caribbean Sea (Saunders & Lea, 2008). In the tropical Pacific, weak but statistically significant negative correlations (less than -0.3) are found in the Niño 3 and Niño 1+2 ($0-10^{\circ}\text{S}$, $90^{\circ}\text{W}-80^{\circ}\text{W}$) regions. This study uses Niño 3 as the domain of remote influence due to its strong negative correlation with Atlantic MDR ACE, a very high correlation with JJASON Niño 1+2 SSTAs ($\rho = 0.89$) and a high degree of predictive skill for Pacific basin-wide ENSO events (Ren et al., 2019).



125

126 **Figure 1:** a) 1950-2020 JJASON correlation between standardized ACE and SSTAs. The blue
 127 box denotes Niño 3 and the red box denotes the Atlantic MDR. Dotted areas indicate the
 128 correlation is statistically significant at the 95% confidence level based on Student's t-test. b)
 129 Standardized time series of ACE and spatially-averaged MDR SSTAs, $\rho = 0.48$. c) Standardized
 130 time series of ACE and spatially-averaged Niño 3 SSTAs, $\rho = -0.30$.

Figures 1b and 1c show the standardized time series of JJASON ACE with respect to the spatially-averaged Atlantic MDR and Niño 3 SSTAs. The positive correlation between ACE and MDR SSTAs ($\rho = 0.48$) is expected (Vimont & Kossin, 2007), as warm MDR SSTAs provide a more favorable environment for TC development. The negative correlation between ACE and Niño 3 SSTAs ($\rho = -0.30$) is consistent with decreased convective activity over the Pacific due to cool tropical Pacific SSTAs, which results in decreased MDR VWS and subsidence, favoring TC formation and intensification (Latif et al., 2007; Vecchi et al., 2008; Wang & Lee, 2008).

While Figure 1 describes a significant influence of both local and remote SSTAs on JJASON ACE, we hypothesize that the early-season interbasin SST relationship may be weighted toward the MDR due to the boreal spring minimum in ENSO variability. In addition, we suggest the role of remote SSTAs is enhanced in the late-season due to the growth of Niño 3 SSTAs associated with the typical ENSO maximum in boreal early-winter. To aid our investigation into the seasonality of interbasin SST influence on Atlantic ACE, we next partition the hurricane season into early-season (JJA) and late-season (SON) periods.

4 Seasonality of Interbasin SST Impacts

Figure 2 shows the correlation between the seasonally-summed ACE and seasonally-averaged SSTAs during JJA and SON. In JJA, the strongest positive correlation is centered in the MDR, which reflects the boreal spring-to-summer dissipating pattern of the AMM (Chiang & Vimont, 2004; Kossin & Vimont, 2007). A statistically significant positive correlation ($\rho = 0.43$) is found between ACE and the spatially-averaged MDR SSTAs. In contrast, there is no significant correlation between Niño 3 SSTAs and ACE during JJA ($\rho = -0.09$). These correlations signify JJA Atlantic TC activity is strongly influenced by local SSTAs, yet weakly influenced by remote SSTAs.

In SON (Figure 2b), the positive correlation between ACE and SSTAs experiences a westward shift towards the Caribbean Sea, consistent with a developing AWP pattern (Wang & Enfield, 2001, 2003). A large area of significant negative correlations between ACE and SSTA is also centered in Niño 3. The correlations between ACE and the MDR and Niño 3 SSTAs are comparable in magnitude ($\rho_{\text{MDR}} = 0.38$ versus $\rho_{\text{Niño 3}} = -0.35$), suggesting the influence of interbasin SSTAs on ACE is weighted evenly in SON between the MDR and Niño 3.

Figure 2c shows the monthly variance for MDR and Niño 3 SSTAs. At the beginning of the hurricane season, Niño 3 variance is at a minimum due to largely neutral ENSO conditions. By boreal autumn, Niño 3 SSTAs exhibit increased variance consistent with the seasonal phase locking of ENSO (Rasmusson & Carpenter, 1982). While MDR SSTAs exhibit less overall variance than Niño 3, a late boreal spring maximum in MDR variance coincides with the spring variance peak of the AMM, which transitions to a minimum through SON (Enfield & Mayer, 1997; Czaja et al., 2002; Czaja, 2004; Chiang & Vimont, 2004). The F-statistic, or the mean monthly variance ratio of MDR versus Niño 3 SSTAs, reveals the interbasin variance of SSTAs is weighted toward Niño 3. The variance of MDR SSTAs is about 30% of Niño 3 in JJA, decreasing to 15% by SON. Together with the correlation results, this variance profile suggests the signal of early-season ACE is weighted towards MDR SSTAs, while late-season ACE is heavily influenced by remote Niño 3 SSTAs due to a stronger SON ENSO teleconnection. This relative SST seasonality will be used to model the distribution of early- and late-season ACE and explore the seasonal predictability of Atlantic TC activity.

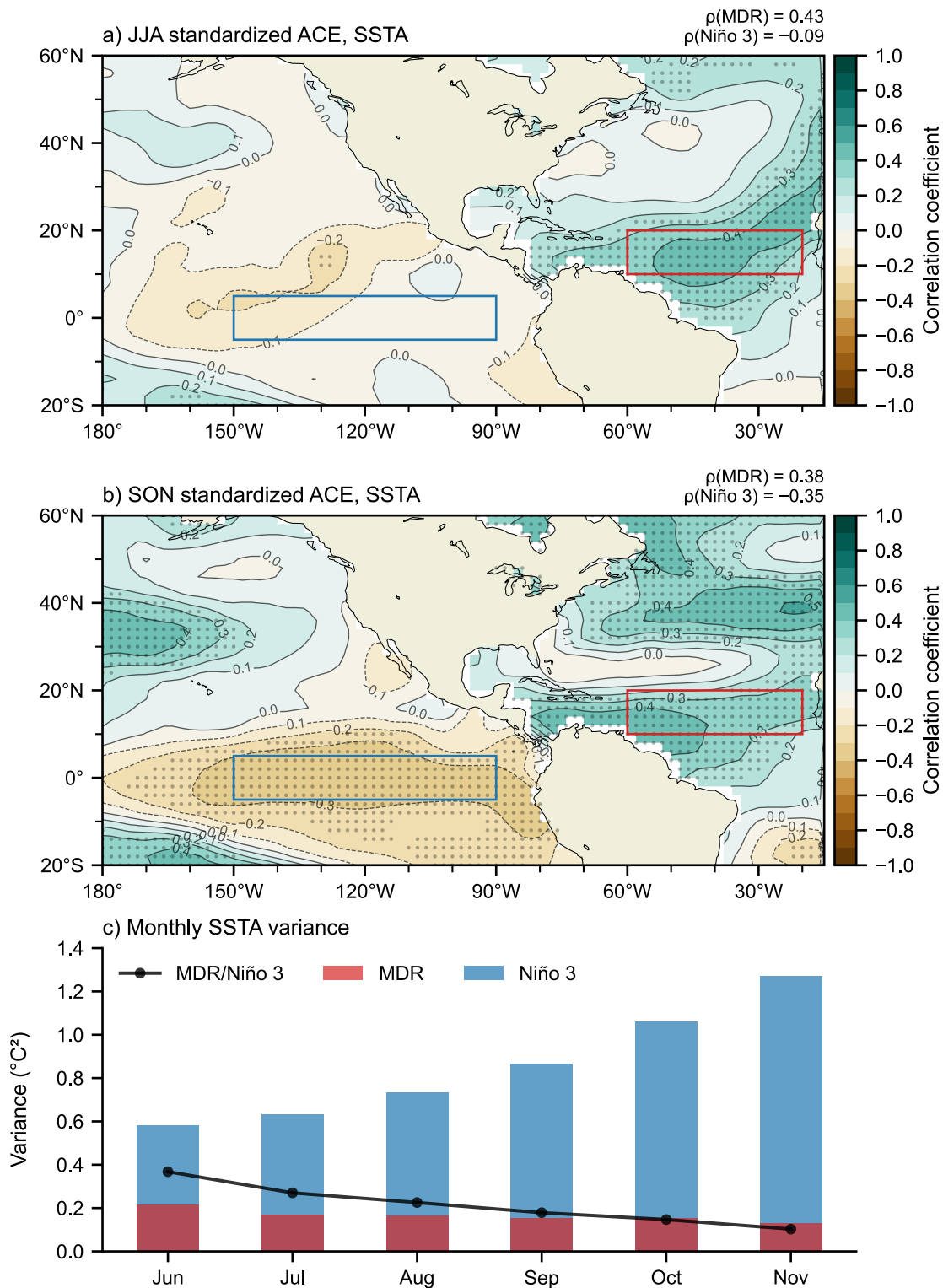


Figure 2: a) JJA and b) SON correlation between standardized ACE and SSTAs, 1950-2020. The blue box denotes Niño 3, the red box denotes the Atlantic MDR and dotted areas indicate the correlation is statistically significant at the 95% confidence level based on Student's t-test.

Correlation coefficients between ACE and the spatially-averaged MDR and Niño 3 SSTAs are given respectively at top right. c) JJASON variance ($^{\circ}\text{C}^2$) during 1950-2020 for spatially-averaged MDR and Niño 3 SSTAs. An F-statistic is obtained from the monthly mean variance ratio of MDR SSTAs to Niño 3 SSTAs and shown by the black line. An F-test at the 95% confidence level finds the monthly variance of the monthly MDR and Niño 3 SSTAs significantly different.

5 The Interbasin SST Index

We construct an interbasin SST index from 71 years (1950-2020) of MDR and Niño 3 ERSSTv5 SSTAs to model the seasonal contributions of local and remote SST to Atlantic TC activity. For JJA and SON, the seasonal cycle is removed and the resulting SSTAs are normalized and area-averaged over the MDR and Niño 3 domains. These SSTAs are then linearly regressed to each respective season's standardized ACE. Figure 3 shows the observed and reconstructed standardized ACE for JJA and SON, where the reconstructed ACE calculated from each season's regression model is referred to as the interbasin index. The observed and reconstructed ACE have a positive JJA correlation of 0.45, but a stronger correlation ($\rho = 0.59$) occurs in SON.

We use a leave-one-out cross validation to assess the predictive skill of the interbasin index relative to linear regression models using only an MDR or Niño 3 SST predictor. The regression models for the interbasin, MDR-only and Niño 3-only cases exclude one year of SST data from the training data set to use for testing the model prediction skill. This is repeated for each year, during which the root mean square error (RMSE) of the forecast relative to observed ACE is calculated. The leave-one-out cross validation results are given in Table S2. The interbasin index has better performance in describing ACE outcomes (RMSE = 0.846, coefficient of determination $R^2 = 0.34$) during SON than an index containing only MDR (RMSE = 0.954, $R^2 = 0.14$) or Niño 3 (RMSE = 0.960, $R^2 = 0.12$) SSTAs. In JJA, the interbasin index has roughly equal skill in predicting TC activity compared to an index using only MDR SSTAs, but an index

of only Niño 3 SSTAs has no skill. This again suggests that the impact of remote Niño 3 SSTAs on Atlantic ACE is minimal in the early-season, yet influential during late-season. In addition, the seasonality of Atlantic TC activity is well represented by the interbasin SST index.

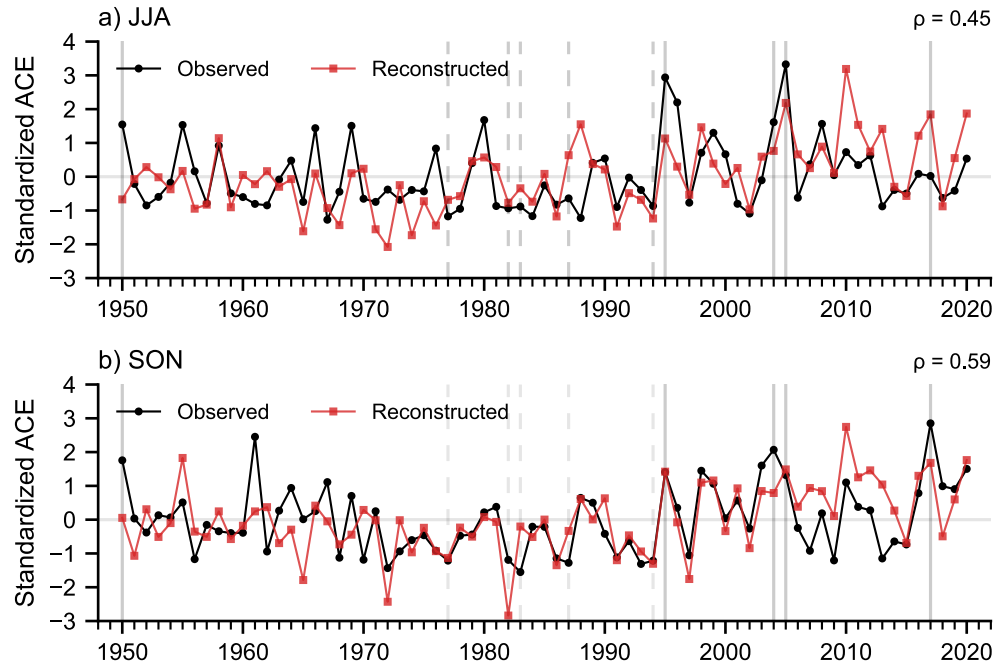


Figure 3: a) JJA and b) SON observed (black) and reconstructed (interbasin SST index, red) standardized ACE, 1950-2020. Solid (dashed) grey vertical lines correspond to the period's five years of largest (smallest) observed ACE. The correlation coefficient between the observed and reconstructed ACE is given at the top right of each panel.

6 Early- and Late-Season Predictability of ACE Using NMME

To further explore whether the interbasin index has skill in predicting early- and late-season Atlantic TC activity, we calculate the JJA and SON interbasin SST indices from 28 years (1982-2009) of NMME hindcast data with May initial conditions, which are coincident with the May release of the NOAA Climate Prediction Center Atlantic Hurricane Season Outlook. The JJA and SON SSTAs for each NMME model ensemble member are computed by removing the seasonal cycle, then normalized by the member's standard deviation and spatially-averaged over the

corresponding region. Each member's standardized MDR and Niño 3 SSTAs are used as predictors in the JJA and SON interbasin indices to forecast a seasonal value of ACE. A NMME superensemble is also computed from the interbasin indices of the eight NMME model ensemble members, where the ensemble mean of each model's forecasted ACE is used as a member of the superensemble. The observed and forecasted ACE values are then divided into terciles to identify the likelihood of an above-, near- or below-normal ACE season. Note that the tercile is computed individually for each model member, which effectively standardizes the variance within the ensemble (i.e., ensemble spread).

We use both deterministic and probabilistic metrics to evaluate the forecast skill of the model. Deterministic methods include anomaly correlation and saturation RMSE, a normalization of the RMSE by the summed variances of the forecast model and observations. Probabilistic skill methods include the relative operating characteristic (ROC) curve, ROC score and the ranked probability skill score (RPSS). Further discussion of the probabilistic skill methods used in this study is found in Supporting Text S1 (see also Swets, 1973; Mason, 1982; Mason & Graham, 1999; Lopez & Kirtman, 2014).

Table S3 provides a summary of the seasonal deterministic and probabilistic forecast scores for each model. All JJA model skills are generally worse than SON, likely due to the reduced potential predictability of Atlantic MDR SST during JJA relative to SON (Becker et al., 2014). Anomaly correlations of each model are lower in JJA than SON except for a small difference in CFSv2, but the RMSE never becomes saturated for any JJA model (approximately 85% error saturation). Negative JJA RPSS values for all models indicate JJA forecasts are similar to climatology (which has an RPSS of 0) when categorically forecasting for either a below-, near- or above-normal ACE season. SON forecasts fare better in the deterministic skill metrics,

241 especially those from CMC2-CanCM4, CESM1 and NASA-GEOSS2S as well as the NMME
242 superensemble. All models have a positive RPSS value in SON, corresponding to categorical
243 forecasts more skilled than climatology, the most skilled being the NMME superensemble.

244 Figures 4a and 4b show JJA and SON ROC curves of below-, near- and above-normal ACE
245 forecasts. In JJA, the below-normal forecasts outperform climatology (i.e., lay above the gray
246 diagonal) while the above-normal forecasts display the greatest skill (i.e., larger ROC score,
247 Table S3). During SON, the below-normal ACE forecast outperforms the above-normal forecast
248 for most NMME models, but both forecast categories show greater probabilistic forecast skill
249 than in JJA. Importantly, the predictability of the highest impact tercile (above-average ACE) is
250 improved in both JJA and SON, with the greatest overall predictability found in the late-season.

251 The reduced forecast skill during JJA with respect to SON may be related to a weaker Atlantic
252 ACE signal in JJA and the decreased variance of Niño 3 SSTAs during the early-season (see
253 Figure 2c and Figure S2). The increasing variance in the remote Pacific basin throughout SON
254 provides a higher signal-to-noise ratio of SSTAs and is more prevalent in model forecasts
255 initialized after the ENSO spring barrier (Lopez & Kirtman, 2014, 2015). However, the early- to
256 late-season reduction in the variance of SSTAs is not seen in the GFDL-CM2 model, which has
257 similar SON prediction skill to other NMME members.

258 Together with earlier results, these forecast skill metrics suggest that the interbasin SST index
259 has utility in predicting both below- and above-normal ACE seasons. The largest skill is found in
260 SON, which coincides with the growth of Niño 3 SSTAs related to the tendency for ENSO to
261 peak in boreal early-winter. Results of the leave-one-out cross validation (Table S2) indicate that
262 the JJA to SON improvement of Niño 3 SSTAs as an ACE predictor also increases the predictive
263 skill of the interbasin index. However, the inclusion of two of the three months that form the

climatological peak of the hurricane season (August-October) in the definition of the late-season likely contributes to the overall increased predictability.

As shown in Figures S3 and S4, the NMME prediction skill for MDR SSTAs is much lower than that of Niño 3 SSTAs, thus serving as a bottleneck for interbasin SST index prediction skill. This suggests that increasing the prediction skill for MDR SSTAs is crucial for improving seasonal outlooks. In addition, it is interesting to note that MDR and Niño 3 SSTAs from ERSSTv5 and NMME are more positively correlated in JJA than in SON, yet this does not translate to increased ACE predictability in JJA relative to SON (Table S3). This indicates that the interbasin SST link to Atlantic TC activity is weaker in JJA than in SON as demonstrated in Figure 3.

7 Summary and Conclusions

Previous studies have described the impacts of local and remote SST on Atlantic TC activity (Latif et al., 2007; Vecchi & Soden, 2007; Swanson, 2008; Vecchi et al., 2008; Wang & Lee, 2008; Lee et al., 2011) and ENSO's role in modulating Atlantic hurricanes (Goldenberg & Shapiro, 1996; Gray, 1984; Shapiro, 1987; Kossin et al., 2010; Klotzbach, 2011). This study explores the influence of interbasin SSTAs on early- and late-season Atlantic TC activity. Our analysis shows that remote Niño 3 SSTAs have little influence on JJA TC activity. This is in agreement with ENSO's phase locking to the seasonal cycle, which corresponds to the growth of remote SSTAs from a minimum in late-spring to a winter maximum (Rasmusson & Carpenter, 1982). However, tropical Pacific convective instability during SON influences vertical wind shear and subsidence over the tropical Atlantic basin, regulating the conditions for TC activity (Gray, 1984; Tang & Neelin, 2004; Lee et al., 2011; Larson et al., 2012). Accordingly, this study describes an enhanced impact of Niño 3 SSTAs on Atlantic TC activity during SON with influence comparable to MDR SSTAs.

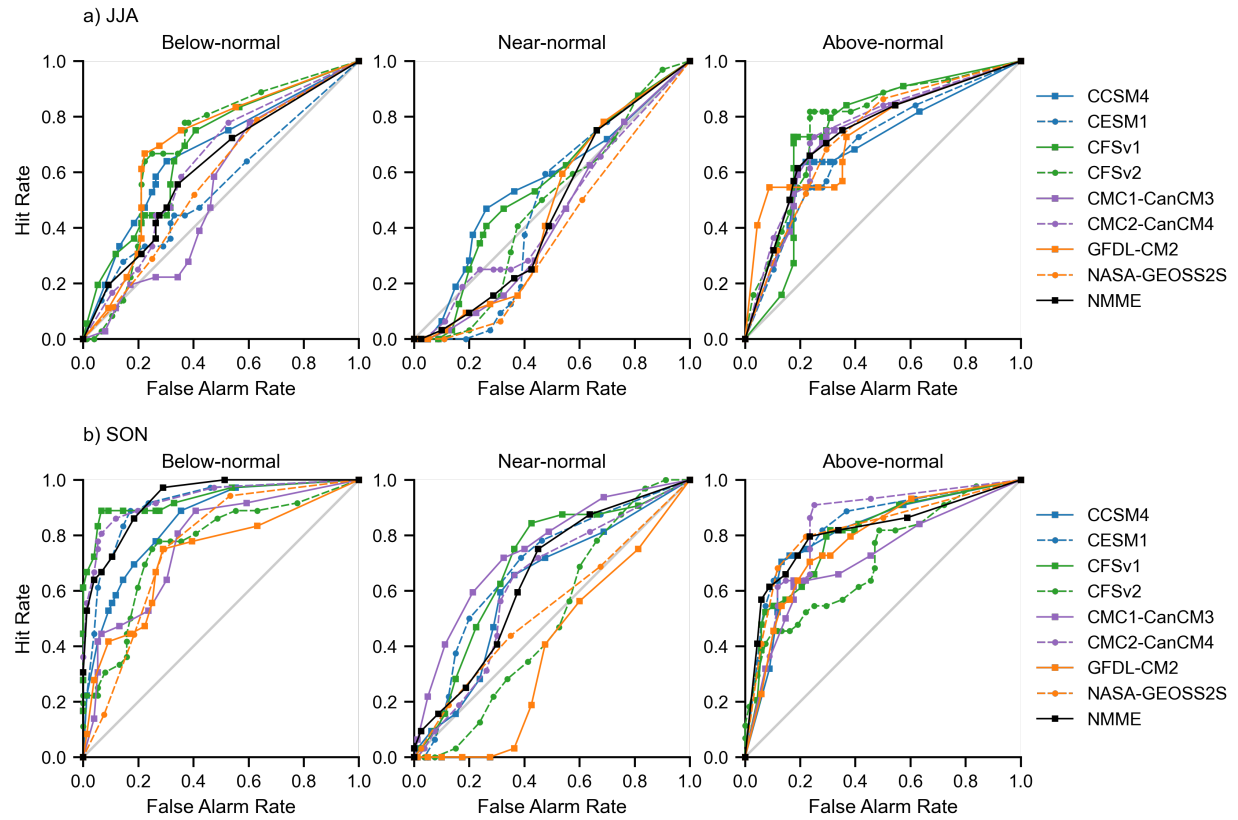


Figure 4: 1982-2009 a) JJA and b) SON ROC curves for below-, near- and above-normal ACE forecasts from the interbasin SST index using NMME model member SST predictors. The colored curves represent NMME model members, the black curve denotes the NMME superensemble and the number of points on a curve corresponds to the number of model ensemble members. The gray diagonal is equivalent to the forecast skill of climatology.

This study finds that MDR SSTAs are of great importance in producing a skillful early-season forecast of ACE while ENSO is not. However, the representation of remote SSTAs, modulated by ENSO, are as important as MDR SSTAs in predicting SON TC activity. NMME ensemble forecasts with May initial conditions can be used to make skillful forecasts of above- and below-average ACE using an interbasin SST index. Notably, this interbasin index provides increased predictability of high-impact TC activity. Despite a longer lead time for the SST predictors in SON than JJA, prediction skills for Atlantic ACE are greater in SON than in JJA, partly because the interbasin SST link to Atlantic TC activity is much weaker in JJA than in SON. Therefore,

there is a need to identify additional predictors for Atlantic ACE, particularly for JJA. Further analysis also indicates that the NMME prediction skill for MDR SSTAs is lower than that of Niño 3 SSTAs, suggesting that increasing the prediction skill for MDR SSTAs is key to improving seasonal outlooks.

Future studies on interbasin teleconnections would benefit from an examination of other TC fields, such as convective available potential energy (CAPE) and VWS, which may shed light on other seasonal characteristics of Atlantic TC activity. The definition of the MDR used in this work might also be extended westward to capture the increased positive correlation between SON SSTAs and ACE in the western Caribbean. Finally, analysis of low frequency SST variability, such as the Atlantic Multidecadal Oscillation or Pacific Decadal Oscillation, may shed light on the applicability of the interbasin SST methodology in representing multidecadal hurricane variability. Developments in these areas would significantly advance the state of operational seasonal hurricane outlooks.

Acknowledgments

The authors thank Sim Aberson for comments that have greatly improved the quality of the manuscript. Robert West was supported by the Northern Gulf Institute (NGI), a NOAA cooperative institute, through the NOAA Oceanic and Atmospheric Research Grant NA16OAR4320199. This research was carried out in part under the auspices of the Cooperative Institute for Marine and Atmospheric Studies (CIMAS), a Cooperative Institute of the University of Miami and the National Oceanic and Atmospheric Administration, cooperative agreement NA20OAR4320472. ERSSTv5 data was provided by the NOAA Physical Sciences Laboratory (PSL) at <https://psl.noaa.gov/data/gridded/data.noaa.ersst.v5.html>. HURDAT2 data was provided by AOML's Hurricane Research Division (HRD) at

https://www.aoml.noaa.gov/hrd/hurdat/Data_Storm.html. NMME model data was provided by the International Research Institute for Climate and Society (IRI) at <http://iridl.ldeo.columbia.edu/SOURCES/Models/.NMME/>.

References

- Becker, E., Dool, H. van den, & Zhang, Q. (2014). Predictability and Forecast Skill in NMME. *Journal of Climate*, 27(15), 5891–5906. <https://doi.org/10.1175/JCLI-D-13-00597.1>
- Bell, G. D., Halpert, M. S., Schnell, R. C., Higgins, R. W., Lawrimore, J., Kousky, V. E., et al. (2000). Climate Assessment for 1999. *Bulletin of the American Meteorological Society*, 81(6), S1–S50. [https://doi.org/10.1175/1520-0477\(2000\)81\[s1:CAF\]2.0.CO;2](https://doi.org/10.1175/1520-0477(2000)81[s1:CAF]2.0.CO;2)
- Camargo, S. J., Ting, M., & Kushnir, Y. (2013). Influence of local and remote SST on North Atlantic tropical cyclone potential intensity. *Climate Dynamics*, 40(5–6), 1515–1529. <https://doi.org/10.1007/s00382-012-1536-4>
- Chiang, J. C. H., & Sobel, A. H. (2002). Tropical Tropospheric Temperature Variations Caused by ENSO and Their Influence on the Remote Tropical Climate. *Journal of Climate*, 15(18), 2616–2631. [https://doi.org/10.1175/1520-0442\(2002\)015<2616:TTVCB>2.0.CO;2](https://doi.org/10.1175/1520-0442(2002)015<2616:TTVCB>2.0.CO;2)
- Chiang, J. C. H., & Vimont, D. J. (2004). Analogous Pacific and Atlantic Meridional Modes of Tropical Atmosphere–Ocean Variability. *Journal of Climate*, 17(21), 4143–4158. <https://doi.org/10.1175/JCLI4953.1>
- Czaja, A., Vaart, P. van der, & Marshall, J. (2002). A Diagnostic Study of the Role of Remote Forcing in Tropical Atlantic Variability. *Journal of Climate*, 15(22), 3280–3290. [https://doi.org/10.1175/1520-0442\(2002\)015<3280:ADSOTR>2.0.CO;2](https://doi.org/10.1175/1520-0442(2002)015<3280:ADSOTR>2.0.CO;2)
- Czaja, A. (2004). Why Is North Tropical Atlantic SST Variability Stronger in Boreal Spring? *Journal of Climate*, 17(15), 3017–3025. [https://doi.org/10.1175/1520-0442\(2004\)017<3017:WINTAS>2.0.CO;2](https://doi.org/10.1175/1520-0442(2004)017<3017:WINTAS>2.0.CO;2)
- Emanuel, K. A. (1994). *Atmospheric convection*. Oxford University Press on Demand.
- Enfield, D. B., & Mayer, D. A. (1997). Tropical Atlantic sea surface temperature variability and its relation to El Niño–Southern Oscillation. *Journal of Geophysical Research: Oceans*, 102(C1), 929–945. <https://doi.org/10.1029/96JC03296>
- Goldenberg, S. B., & Shapiro, L. J. (1996). Physical Mechanisms for the Association of El Niño and West African Rainfall with Atlantic Major Hurricane Activity. *Journal of Climate*, 9(6), 1169–1187. [https://doi.org/10.1175/1520-0442\(1996\)009<1169:PMFTAO>2.0.CO;2](https://doi.org/10.1175/1520-0442(1996)009<1169:PMFTAO>2.0.CO;2)
- Goldenberg, S. B., Landsea, C. W., Mestas-Núñez, A. M., & Gray, W. M. (2001). The Recent Increase in Atlantic Hurricane Activity: Causes and Implications. *Science*, 293(5529), 474–479. <https://doi.org/10.1126/science.1060040>

- Gray, W. M. (1968). Global View of the Origin of Tropical Disturbances and Storms. *Monthly Weather Review*, 96(10), 669–700. [https://doi.org/10.1175/1520-0493\(1968\)096<0669:GVOTOO>2.0.CO;2](https://doi.org/10.1175/1520-0493(1968)096<0669:GVOTOO>2.0.CO;2)
- Gray, W. M. (1984). Atlantic Seasonal Hurricane Frequency. Part I: El Niño and 30 mb Quasi-Biennial Oscillation Influences. *Monthly Weather Review*, 112(9), 1649–1668. [https://doi.org/10.1175/1520-0493\(1984\)112<1649:ASHFPI>2.0.CO;2](https://doi.org/10.1175/1520-0493(1984)112<1649:ASHFPI>2.0.CO;2)
- Huang, B., Thorne, P. W., Banzon, V. F., Boyer, T., Chepurin, G., Lawrimore, J. H., et al. (2017). Extended Reconstructed Sea Surface Temperature, Version 5 (ERSSTv5): Upgrades, Validations, and Intercomparisons. *Journal of Climate*, 30(20), 8179–8205. <https://doi.org/10.1175/JCLI-D-16-0836.1>
- Kirtman, B. P., Min, D., Infanti, J. M., Kinter, J. L., Paolino, D. A., Zhang, Q., et al. (2014). The North American Multimodel Ensemble: Phase-1 Seasonal-to-Interannual Prediction; Phase-2 toward Developing Intraseasonal Prediction. *Bulletin of the American Meteorological Society*, 95(4), 585–601. <https://doi.org/10.1175/BAMS-D-12-00050.1>
- Klotzbach, P. J. (2011). El Niño–Southern Oscillation’s Impact on Atlantic Basin Hurricanes and U.S. Landfalls. *Journal of Climate*, 24(4), 1252–1263. <https://doi.org/10.1175/2010JCLI3799.1>
- Knutson, T., Camargo, S. J., Chan, J. C. L., Emanuel, K., Ho, C.-H., Kossin, J., et al. (2020). Tropical Cyclones and Climate Change Assessment: Part II: Projected Response to Anthropogenic Warming. *Bulletin of the American Meteorological Society*, 101(3), E303–E322. <https://doi.org/10.1175/BAMS-D-18-0194.1>
- Kossin, J. P., & Vimont, D. J. (2007). A More General Framework for Understanding Atlantic Hurricane Variability and Trends. *Bulletin of the American Meteorological Society*, 88(11), 1767–1782. <https://doi.org/10.1175/BAMS-88-11-1767>
- Kossin, J. P., Camargo, S. J., & Sitkowski, M. (2010). Climate Modulation of North Atlantic Hurricane Tracks. *Journal of Climate*, 23(11), 3057–3076. <https://doi.org/10.1175/2010JCLI3497.1>
- Landsea, C. W. (1993). A Climatology of Intense (or Major) Atlantic Hurricanes. *Monthly Weather Review*, 121(6), 1703–1713. [https://doi.org/10.1175/1520-0493\(1993\)121<1703:ACOIMA>2.0.CO;2](https://doi.org/10.1175/1520-0493(1993)121<1703:ACOIMA>2.0.CO;2)
- Landsea, C. W. (2007). Counting Atlantic tropical cyclones back to 1900. *Eos, Transactions American Geophysical Union*, 88(18), 197–202. <https://doi.org/10.1029/2007EO180001>
- Landsea, C. W., & Franklin, J. L. (2013). Atlantic Hurricane Database Uncertainty and Presentation of a New Database Format. *Monthly Weather Review*, 141(10), 3576–3592. <https://doi.org/10.1175/MWR-D-12-00254.1>
- Larson, S., Lee, S.-K., Wang, C., Chung, E.-S., & Enfield, D. B. (2012). Impacts of non-canonical El Niño patterns on Atlantic hurricane activity. *Geophysical Research Letters*, 39(14). <https://doi.org/10.1029/2012GL052595>
- Latif, M., Keenlyside, N., & Bader, J. (2007). Tropical sea surface temperature, vertical wind shear, and hurricane development. *Geophysical Research Letters*, 34(1). <https://doi.org/10.1029/2006GL027969>

- 401 Lee, S.-K., Enfield, D. B., & Wang, C. (2011). Future Impact of Differential Interbasin Ocean
402 Warming on Atlantic Hurricanes. *Journal of Climate*, 24(4), 1264–1275.
403 <https://doi.org/10.1175/2010JCLI3883.1>
- 404 Lopez, H., & Kirtman, B. P. (2014). WWBs, ENSO predictability, the spring barrier and extreme
405 events. *Journal of Geophysical Research: Atmospheres*, 119(17), 10,114–10,138.
406 <https://doi.org/10.1002/2014JD021908>
- 407 Lopez, H., & Kirtman, B. P. (2015). Tropical Pacific internal atmospheric dynamics and
408 resolution in a coupled GCM. *Climate Dynamics*, 44(1), 509–527.
409 <https://doi.org/10.1007/s00382-014-2220-7>
- 410 Mason, I. (1982). A model for assessment of weather forecasts. *Australian Meteorological*
411 *Magazine*, 30(4), 291–303.
- 412 Mason, S. J., & Graham, N. E. (1999). Conditional Probabilities, Relative Operating
413 Characteristics, and Relative Operating Levels. *Weather and Forecasting*, 14(5), 713–
414 725. [https://doi.org/10.1175/1520-0434\(1999\)014<0713:CPROCA>2.0.CO;2](https://doi.org/10.1175/1520-0434(1999)014<0713:CPROCA>2.0.CO;2)
- 415 Rasmusson, E. M., & Carpenter, T. H. (1982). Variations in Tropical Sea Surface Temperature
416 and Surface Wind Fields Associated with the Southern Oscillation/El Niño. *Monthly*
417 *Weather Review*, 110(5), 354–384. [https://doi.org/10.1175/1520-0493\(1982\)110<0354:VITSST>2.0.CO;2](https://doi.org/10.1175/1520-0493(1982)110<0354:VITSST>2.0.CO;2)
- 419 Ren, H.-L., Zuo, J., & Deng, Y. (2019). Statistical predictability of Niño indices for two types of
420 ENSO. *Climate Dynamics*, 52(9), 5361–5382. [https://doi.org/10.1007/s00382-018-4453-](https://doi.org/10.1007/s00382-018-4453-3)
421 3
- 422 Saunders, M. A., & Lea, A. S. (2008). Large contribution of sea surface warming to recent
423 increase in Atlantic hurricane activity. *Nature*, 451(7178), 557–560.
424 <https://doi.org/10.1038/nature06422>
- 425 Shapiro, L. J. (1987). Month-to-Month Variability of the Atlantic Tropical Circulation and Its
426 Relationship to Tropical Storm Formation. *Monthly Weather Review*, 115(11), 2598–
427 2614. [https://doi.org/10.1175/1520-0493\(1987\)115<2598:MTMVOT>2.0.CO;2](https://doi.org/10.1175/1520-0493(1987)115<2598:MTMVOT>2.0.CO;2)
- 428 Swanson, K. L. (2008). Nonlocality of Atlantic tropical cyclone intensities. *Geochemistry,*
429 *Geophysics, Geosystems*, 9(4). <https://doi.org/10.1029/2007GC001844>
- 430 Swets, J. A. (1973). The Relative Operating Characteristic in Psychology: A technique for
431 isolating effects of response bias finds wide use in the study of perception and cognition.
432 *Science*, 182(4116), 990–1000. <https://doi.org/10.1126/science.182.4116.990>
- 433 Tang, B. H., & Neelin, J. D. (2004). ENSO Influence on Atlantic hurricanes via tropospheric
434 warming. *Geophysical Research Letters*, 31(24). <https://doi.org/10.1029/2004GL021072>
- 435 Vecchi, G. A., & Soden, B. J. (2007). Effect of remote sea surface temperature change on
436 tropical cyclone potential intensity. *Nature*, 450(7172), 1066–1070.
437 <https://doi.org/10.1038/nature06423>
- 438 Vecchi, G. A., Swanson, K. L., & Soden, B. J. (2008). Whither Hurricane Activity? *Science*,
439 322(5902), 687–689. <https://doi.org/10.1126/science.1164396>

- Vimont, D. J., & Kossin, J. P. (2007). The Atlantic Meridional Mode and hurricane activity. *Geophysical Research Letters*, 34(7). <https://doi.org/10.1029/2007GL029683>
- Wang, C., & Enfield, D. B. (2001). The Tropical Western Hemisphere Warm Pool. *Geophysical Research Letters*, 28(8), 1635–1638. <https://doi.org/10.1029/2000GL011763>
- Wang, C., & Enfield, D. B. (2003). A Further Study of the Tropical Western Hemisphere Warm Pool. *Journal of Climate*, 16(10), 1476–1493. [https://doi.org/10.1175/1520-0442\(2003\)016<1476:AFSOTT>2.0.CO;2](https://doi.org/10.1175/1520-0442(2003)016<1476:AFSOTT>2.0.CO;2)
- Wang, C., & Fiedler, P. C. (2006). ENSO variability and the eastern tropical Pacific: A review. *Progress in Oceanography*, 69(2–4), 239–266. <https://doi.org/10.1016/j.pocean.2006.03.004>
- Wang, C., & Lee, S.-K. (2008). Global warming and United States landfalling hurricanes. *Geophysical Research Letters*, 35(2). <https://doi.org/10.1029/2007GL032396>
- Wang, C., Enfield, D. B., Lee, S.-K., & Landsea, C. W. (2006). Influences of the Atlantic Warm Pool on Western Hemisphere Summer Rainfall and Atlantic Hurricanes. *Journal of Climate*, 19(12), 3011–3028. <https://doi.org/10.1175/JCLI3770.1>
- Xie, L., Yan, T., Pietrafesa, L. J., Morrison, J. M., & Karl, T. (2005). Climatology and Interannual Variability of North Atlantic Hurricane Tracks. *Journal of Climate*, 18(24), 5370–5381. <https://doi.org/10.1175/JCLI3560.1>
- Yulaeva, E., & Wallace, J. M. (1994). The Signature of ENSO in Global Temperature and Precipitation Fields Derived from the Microwave Sounding Unit. *Journal of Climate*, 7(11), 1719–1736. [https://doi.org/10.1175/1520-0442\(1994\)007<1719:TSEOIG>2.0.CO;2](https://doi.org/10.1175/1520-0442(1994)007<1719:TSEOIG>2.0.CO;2)
- Zhang, R., & Delworth, T. L. (2006). Impact of Atlantic multidecadal oscillations on India/Sahel rainfall and Atlantic hurricanes. *Geophysical Research Letters*, 33(17). <https://doi.org/10.1029/2006GL026267>